BMC Biology

RESEARCH ARTICLE Open Access

Phospho-code of a conserved transcriptional factor underpins fungal virulence

Jiyun Yang[1†], Bing Li[2*†], Yu-Ting Pan[1], Ping Wang[1], Mei-Ling Sun[1], Ki-Tae Kim[3], Hui Sun[1], Jian-Ren Ye[1], Zhen Jiao[2], Yong-Hwan Lee[4] and Lin Huang[1*]

Abstract

Background Cell wall integrity (CWI) is crucial for fungal growth, pathogenesis, and adaptation to extracellular environments. Calcofluor white (CFW) is a cell wall perturbant that inhibits fungal growth, yet little is known about how phytopathogenic fungi respond to the CFW-induced stress.

Results In this study, we unveiled a significant discovery that CFW triggered the translocation of the transcription factor CgCrzA from the cytoplasm to the nucleus in *Colletotrichum gloeosporioides*. This translocation was regulated by an interacting protein, CgMkk1, a mitogen-activated protein kinase involved in the CWI pathway. Further analysis revealed that CgMkk1 facilitated nuclear translocation by phosphorylating CgCrzA at the Ser280 residue. Using chromatin immunoprecipitation sequencing, we identified two downstream targets of CgCrzA, namely *CgCHS5* and *CgCHS6*, which are critical for growth, cell wall integrity, and pathogenicity as chitin synthase genes.

Conclusions These findings provide a novel insight into the regulatory mechanism of CgMkk1-CgCrzA-CgChs5/6, which enables response of the cell wall inhibitor CFW and facilitates infectious growth for *C. gloeosporioides*.

Keywords Calcofluor white CFW, Transcription factor CgCrzA, Mitogen-activated protein kinase CgMkk1, Phosphorylation, Cell wall integrity, Pathogenicity, Chitin synthases

Background

The fungal cell wall is critical for maintaining hyphal shape and adapting to the environment throughout the cell cycle [1]. Its composition varies among species and is composed of chitin and α-(1,3)-glucan in fungi, surrounded by β-glucans and glycoproteins [1, 2]. In plants, pectin, cellulose, and lignin can influence the extensibility and porosity of the cell wall, with lignin providing protection against the cell from environmental challenges [3, 4]. Similarly, the fungal cell wall serves as a shield against various stressors and can elicit host immune response in mammals and plants [5, 6]. Consequently, maintaining cell wall integrity (CWI) is crucial for fungal development and pathogenesis [5].

The CWI pathway represents a critical response mechanism in the budding yeast *Saccharomyces cerevisiae* and other fungi, reacting to both internal and external cues [7]. The key components of the CWI pathway in *S. cerevisiae*, include Bck1, Mkk1, Mkk2, Mpk1, and Slt2 [8]. Disrupting any of these components results in cell lysis [9]. In *Colletotrichum gloeosporioides*, the MAPK pathway, involving the components

†Jiyun Yang and Bing Li contributed equally to this work.

*Correspondence:
Bing Li
006805@yzu.edu.cn
Lin Huang
lhuang@njfu.edu.cn
[1] Co-Innovation Center for Sustainable Forestry in Southern China, Nanjing Forestry University, Nanjing, Jiangsu 210037, China
[2] School of Agricultural Sciences, Zhengzhou University, Zhengzhou, Henan 450001, China
[3] Department of Agricultural Life Science, Sunchon National University, Suncheon 57922, Korea
[4] Department of Agricultural Biotechnology, Seoul National University, Seoul 08826, Korea

such as CgMck1 (the Bck1 homologue) and CgMkk1, plays pivotal role in vegetative growth, asexual development, CWI, stressors resistance, and infection morphogenesis [10]. Similarly, in *Magnaporthe oryzae*, MoMck1 and MoMps1 are necessary for CWI and pathogenicity [9, 11]. Yin et al. found that MoAtg1 can phosphorylate MoMkk1 in response to endoplasmic reticulum stress in *M. oryzae* [12]. These findings emphasize the significance of CWI signal transmission in fungal development and pathogenicity.

Chitin is a major structural component of the fungal cell wall that is synthesized by chitin synthase (CHS) [13]. Typically, filamentous fungi contain seven to eight *CHS* genes with their functional extensively characterized in fungi such as *Aspergillus nidulans*, *M. oryzae*, *Neurospora crassa*, and *Ustilago maydis* [14–17]. In *M. oryzae*, seven *CHS* genes have been identified, with mutants of *CHS1, CHS6,* and *CHS7*, displaying significantly reduced virulence [14]. Conversely, in *U. maydis*, while *CHS1* and *CHS2* appear to have no obvious effect on mating, virulence, or dimorphic behavior, *CHS5*, *CHS6*, and *CHS7* are crucial for virulence [17]. These findings suggest varying roles for different chitin synthases in the development and pathogenesis of filamentous fungi.

Transcription factors play crucial roles in regulating gene expression, development, metabolism, and response to environmental stimuli [18]. The calcineurin-responsive transcription factor Crz1, a member of the zinc-finger protein family, is involved in cell wall integrity maintenance, ionic homeostasis, stress response in *S. cerevisiae* [19]. In *C. gloeosporioides*, CgCrzA (the Crz1 homologue) has been shown to regulate various processes, including hyphal growth, conidiogenesis, appressorial formation, pathogenicity, cell wall biosynthesis, and expression of *CHS* genes [20, 21]. When exposed to Ca^{2+}, CgCrzA can translocate from the cytoplasm to the nucleus [21]. This study revealed that exposure to Calcofluor White (CFW) induces the translocation of CgCrzA from the cytoplasm to the nucleus. To better understand the response of *C. gloeosporioides* to CFW stress and the activation of downstream genes, we aimed to identify the upstream kinase regulating CgCrzA in response to CFW. Our findings show that exposure to CFW activates the CWI MAPK cascade, leading to the interaction and phosphorylation of CgCrzA by CgMkk1, thereby promoting CgCrzA translocation to the nucleus. Furthermore, we discovered that the phosphorylated CgCrzA activates the transcription of *CgCHS5/6*, key components of the CWI pathway. These results provide novel insights into the regulatory mechanisms of the CWI pathway in *C. gloeosporioides*.

Results

CgCrzA translocates from the cytoplasm to the nucleus under CFW conditions

To further explore the mechanism of CWI maintenance by CrzA, we initially studied the subcellular localization of CgCrzA in response to the cell wall biosynthesis inhibitor CFW. In liquid CM culture, CgCrzA exhibited an even distribution in the cytoplasm and nucleus. However, upon treatment with CFW for 60 min, there was a significant increase in nuclear localization of CgCrzA-GFP (63.56 ± 13.25%) (Fig. 1A). Extending the CFW treatment duration to 120 min resulted in nearly complete nuclear localization of CgCrzA-GFP (92.31 ± 18.14%). No observable CgCrzA-GFP signal remained in the cytoplasmic of CFW-treated hyphae (Fig. 1A). This increased nuclear localization of CgCrzA-GFP was further validated by co-expression with a red fluorescent protein fused with histone H1 (CgH1-RFP, serving as a nuclear-locational marker protein) (Fig. 1A). Additionally, chromatin fractionation revealed a significant increase in nuclear localization of CgCrzA under CFW conditions, while the cytoplasm fraction of CgCrzA-GFP in hyphae showed a pronounced decrease, as confirmed by immunoblotting using anti-GFP antibodies (Fig. 1B, C).

CgMkk1 interacts with CgCrzA, and is involved in the development, CWI, and virulence of *C. gloeosporioides*

We found that CgMkk1, a pivotal regulator within MAPK cascade pathway, robustly interacted with CgCrzA both in vitro and in *vivo*, as demonstrated by yeast two-hybrid (Y2H) and co-immunoprecipitation (co-IP) assays (Fig. 1D, E). To investigate the impact of CgMKK1 deletion on CgCrzA distribution and CWI, we generated a Δ*Cgmkk1* mutant. The data showed a significant decrease in the growth rate of the Δ*Cgmkk1* mutant, displaying similar characteristics to those of the Δ*CgcrzA* mutant (Additional file 1, Fig. S1A, B). Additionally, the Δ*Cgmkk1* mutant exhibited a notable decrease in conidiation compared to the wild-type and complemented strains (Additional file 1, Fig. S1C), mirroring the deficiency observed in the Δ*CgcrzA* mutant. Pathogenicity analysis also showed that the Δ*Cgmkk1* mutant displayed impaired virulence (Additional file 1, Fig. S1D).

Chitin staining was employed to assess cell wall properties, revealing altered chitin distribution in the Δ*Cgmkk1* mutant in comparison to the wild-type (Additional file 1, Fig. S2A). The fluorescence signals were mainly localized at the hyphal tips in the wild-type. However, in the Δ*Cgmkk1* mutant, the fluorescence signals were not only restricted to the hyphal tips, but also distributed in the lateral walls (Additional file 1, Fig. S2A). Furthermore, treatment of

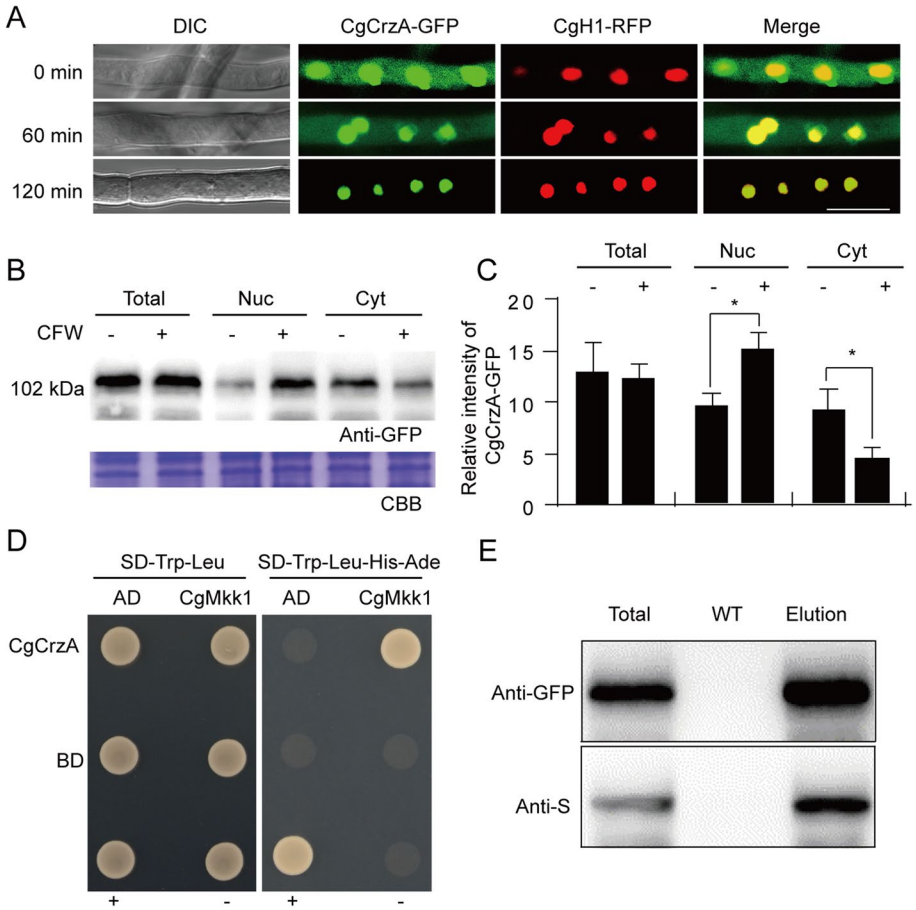

Fig. 1 Nuclear translocation of CgCrzA and its interaction with CgMkk1 under CFW stress. **A** Localisation of CgCrzA under CFW stress was examined by observing mycelia treated with CFW for 60 and 120 min using confocal fluorescence microscopy. Scale bar = 10 μm. **B** Five grams of mycelia (untreated and treated with CFW for 60 min) was divided into three parts to extract total protein, nuclear protein, and cytoplasm protein. SDS-PAGE was used to separate proteins, followed by western blotting with an anti-GFP antibody to detect CgCrzA. Bands corresponding to CgCrzA-GFP were observed at 102 kDa. CBB, Coomassie Brilliant Blue. **C** Grayscale analysis was performed on the western blot bands to analyze their intensities. The intensity of CgCrzA was compared between untreated (-) and CFW-treated (+) mycelia (60 min) for total, nuclear, and cytoplasmic proteins. Error bars represent the standard errors from three independent experiments. Asterisks indicate a significant difference at $P < 0.01$. **D** Yeast two-hybrid assays for the interaction between CgMkk1 and CgCrzA. The prey and bait constructs were assayed for growth on SD-Leu-Trp and SD-Leu-Trp-His-Ade plates. "+" denotes positive control, while "-" represents negative control. **E** Co-immunoprecipitation assays for the interaction between CgMkk1 and CgCrzA. Total proteins were isolated from transformants co-expressing CgMkk1-S and CgCrzA-GFP constructs, and proteins eluted from the anti-GFP beads (elution). Immunoblots were incubated with monoclonal anti-GFP and anti-S antibodies

mycelia with cell wall-degrading enzymes resulted in a higher release of protoplasts from the Δ*Cgmkk1* mutant compared to the wild-type and complemented strains (Additional file 1, Fig. S2B, C). Moreover, the chitin content of hypha in the Δ*Cgmkk1* mutant was reduced by 60% compared to the wild-type and complemented strains (Additional file 1, Fig. S2D). The Δ*Cgmkk1* mutant exhibited increased sensitivity to the cell wall perturbant Congo Red and CFW (Additional file 1, Fig. S3A, B).

CgMkk1-dependent phosphorylation of CgCrzA governs its localisation

Our data revealed an interaction between CgCrzA and CgMkk1, the latter being a kinase. Thus, we hypothesized that interaction might involve the phosphorylation of CgCrzA by CgMkk1. To test this hypothesis, we conducted Mn^{2+}-Phos-tag assays, which showed a distinct band shift of CgCrzA-GFP in the wild-type strain following 120 min of CFW treatment (Fig. 2A). Notably, no phosphorylation of CgCrzA-GFP was observed

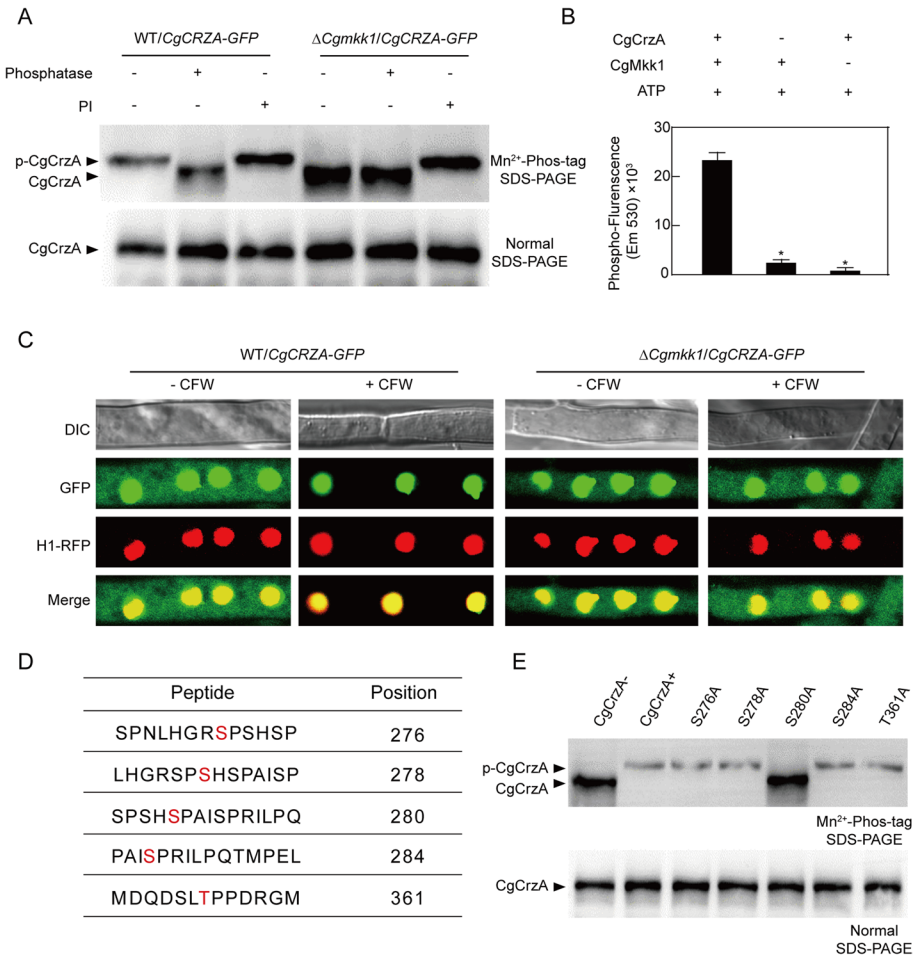

Fig. 2 CgMkk1-mediated phosphorylation and localisation of CgCrzA under CFW Stress. **A** In vivo phosphorylation of CgCrzA by CgMkk1 detected using Mn^{2+}-Phos-tag and conventional SDS-PAGE gel, with detection facilitated by an anti-GFP antibody. Phosphatase represents alkaline phosphatase treatment; PI indicates phosphatase inhibitors. **B** In vitro phosphorylation analysis conducted using the FDIT method. Error bars represent standard deviation. Asterisks indicate a significant difference at $P < 0.01$. **C** Localization of CgCrzA in the Δ*Cgmkk1* mutant observed in response to CFW. Scale Bar = 10 μm. **D** LC-MS/MS analysis identified CgCrzA phosphorylation sites in the wild-type and Δ*Cgmkk1* mutant expressing CgCrzA. **E** In vivo phosphorylation of CgCrzA by CgMkk1 is abolished upon mutation of the Ser280 residue. Variants of CgCrzA expressed in Δ*CgcrzA* and their phosphorylation level in response to CFW were detected using Mn^{2+}-Phos-tag (upper) and normal SDS-PAGE (lower) gel

in the Δ*Cgmkk1*/*CgCRZA-GFP* after CFW treatment, resembling the characteristics of phosphatase treatment (Fig. 2A). In the control experiment, a similar band shift was observed between the WT/ *CgCRZA-GFP* and Δ*Cgmkk1*/ *CgCRZA-GFP* strains (Fig. 2A).

To further substantiate the phosphorylation of CgCrzA by CgMkk1, we conducted Phos-Fluorescence assays using purified His-CgCrzA proteins from *Escherichia coli* strain *BL21*, incubated with GST-CgMkk1. The presence of GST-CgMkk1 led to a stronger Phos-Fluorescence signal compared to its absence (Fig. 2B). Moreover, CgCrzA-GFP was localized in both the cytoplasm and nucleus in the wild-type and Δ*Cgmkk1* mutant under normal conditions (Fig. 2C). When treated with CFW, CgCrzA-GFP translocated from the cytoplasm to the nucleus in the wild-type strain, while CgCrzA-GFP remained in the cytoplasm instead of translocating into nucleus in the Δ*Cgmkk1* mutant (Fig. 2C). These results indicated that CgMkk1-mediated phosphorylation translocated CgCrzA into nucleus.

Furthermore, LC-MS/MS analysis identified potential phosphorylation sites, including S276, S278, S280, S284, and T361, but none of these sites were found in the Δ*Cgmkk1* mutant strain (Fig. 2D). To further validate the accurate amino acid phosphorylated by CgMkk1, we mutated CgCrzA Ser-276, -278, -280, -284, and -T361 to Ala, linked these proteins with GFP, and expressed them in the Δ*Cgmkk1* mutant strain, respectively. We found

that only the band for CgCrzA^{S280A} shifted as rapidly as the bands of the bands of the control and other mutant strains (Fig. 2E), indicating that CgCrzA^{S280A}-GFP is an unphosphorylated protein, and that CgCrzA Ser280 is a specific site for CgMkk1-mediated phosphorylation under CFW conditions (Fig. 2E).

The function of CgCrzA relies on phosphorylation at Ser280

To investigate the role of Ser280 phosphorylation, we examined the phenotypes of phosphomimetic (S280D) and phosphor-dead (S280A) mutant strains. These results revealed that vegetative growth, pathogenicity, and cell wall integrity defects were partially suppressed by the phosphorylation site mutation alleles. The mutant with constitutively phosphorylated site exhibited growth and virulence similar to the wild-type, whereas the phosphor-dead mutant (Δ*CgcrzA*/*CgCRZA*^{S280A}) displayed slower growth and weaker virulence, compared to both the wild-type and Δ*CgcrzA*/*CgCRZA*^{S280D} strains (Fig. 3A and Additional file 1, Fig. S4A).

Furthermore, we assessed the effects of constitutively phosphorylated and dephosphorylated CgCrzA on cell wall integrity of *C. gloeosporioides*. Chitin staining revealed uneven chitin distribution and a lack of concentration at the growing apices in the constitutively dephosphorylated mutant, similar to that in the Δ*CgcrzA* mutant (Fig. 3C). To corroborate the impact on the cell wall of Δ*CgcrzA*/*CgCRZA*^{S280A} and Δ*CgcrzA*/*CgCRZA*^{S280D} strains, we tested the susceptibility of cell wall to cell wall-degrading enzymes. We observed that the hypha of the constitutively dephosphorylated Δ*CgcrzA*/*CgCRZA*^{S280A} mutant released more protoplasts than those of the Δ*CgcrzA*/*CgCRZA*^{S280D} mutant and wild-type, suggesting increased sensitivity (Fig. 3E). Additionally, the Δ*CgcrzA*/*CgCRZA*^{S280A} strains were more susceptible to cell wall stressors CFW and Congo Red (CR) than the Δ*CgcrzA* mutant (Fig. 3G). These results suggest that CgCrzA phosphorylation by CgMkk1 positively regulates the CWI in *C. gloeosporioides*.

Constitutively phosphorylated CgCrzA recovers the defects in Δ*Cgmkk1*

To further investigate whether phosphorylation of CgCrzA at Ser280 could rescue the phenotype of Δ*Cgmkk1* mutant, the transformants of Δ*Cgmkk1*/*CgCRZA*^{S280A} and Δ*Cgmkk1*/*CgCRZA*^{S280D} were generated. Phenotypic analyses revealed that *CgCRZA*^{S280D} partially recovered the defects of vegetative growth on PCA and CM plates, while the growth of Δ*Cgmkk1*/*CgCRZA*^{S280A} transformant remained similar to that of the Δ*Cgmkk1* mutant (Additional file 1, Fig. S4B). Pathogenicity assay also showed that Δ*Cgmkk1*/*CgCRZA*^{S280D} mutant exhibited partial recovery in virulence, whereas Δ*Cgmkk1*/*CgCRZA*^{S280A}, like Δ*Cgmkk1*, failed to infect wounded leaves of *C. lanceolata* (Fig. 3B).

We also assessed the effect of constitutively phosphorylated or dephosphorylated CgCrzA on CWI defects in the

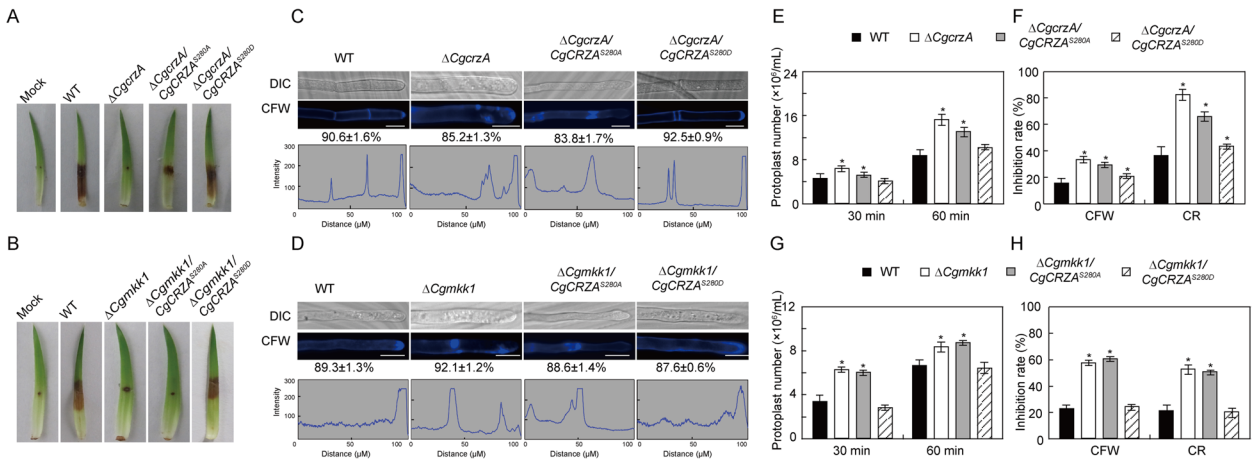

Fig. 3 Vital roles of CgCrzA phosphorylation at Ser280 in virulence and cell wall integrity. **A**, **B** Disease lesions on wounded leaves of *C. lanceolate*, caused by the wild-type, Δ*CgcrzA*, Δ*CgcrzA*/*CgCRZA*^{S280A}, Δ*cgcrzA*/*CgCRZA*^{S280D}, Δ*Cgmkk1*, Δ*Cgmkk1*/*CgCRZA*^{S280A}, and Δ*Cgmkk1*/*CgCRZA*^{S280D} strains at 5 days post-inoculation with conidial suspensions. **C**, **D** Chitin staining with CFW in the hyphae of the wild-type, Δ*CgcrzA*, Δ*CgcrzA*/*CgCRZA*^{S280A}, Δ*cgcrzA*/*CgCRZA*^{S280D}, Δ*Cgmkk1*, Δ*Cgmkk1*/*CgCRZA*^{S280A}, and Δ*Cgmkk1*/*CgCRZA*^{S280D} strains. Bar = 10 μm. **E**, **F** Statistical analysis of protoplast release from the wild-type, Δ*CgcrzA*, Δ*CgcrzA*/*CgCRZA*^{S280A}, Δ*CgcrzA*/*CgCRZA*^{S280D}, Δ*Cgmkk1*, Δ*Cgmkk1*/*CgCRZA*^{S280A}, and Δ*Cgmkk1*/*CgCRZA*^{S280D} strains after treatment with cell wall-degrading enzymes. **G**, **H** Growth inhibition ratio of the wild-type, Δ*CgcrzA*, Δ*CgcrzA*/*CgCRZA*^{S280A}, Δ*CgcrzA*/*CgCRZA*^{S280D}, Δ*Cgmkk1*, Δ*Cgmkk1*/*CgCRZA*^{S280A}, and Δ*Cgmkk1*/*CgCRZA*^{S280D} subjected to CFW and CR, respectively. Error bars represent standard deviation. Asterisks indicate a significant difference at $P < 0.01$

Δ*Cgmkk1* mutant. Consistent with previous findings, the Δ*Cgmkk1* mutant showed defects in chitin distribution, which could be rescued by expressing constitutively phosphorylated CgCrzA (Fig. 3D). Protoplast release experiment showed that the Δ*Cgmkk1*/*CgCRZA*^{S280A} mutant released more protoplasts than the Δ*Cgmkk1*/*CgCRZA*^{S280D} mutant and wild-type (Fig. 3G). Moreover, Δ*Cgmkk1*/*CgCRZA*^{S280D} exhibited stronger resistance against the cell wall inhibitors CFW and CR compared to the Δ*Cgmkk1* mutant (Fig. 3H).

Genome-wide identification of direct downstream target genes to CgCrzA

Chromatin immunoprecipitation followed by sequencing (ChIP-seq) analysis was performed to evaluate whether CgCrzA plays a role in regulating CWI-related genes. Compared to the control, the ChIP-seq samples exhibited enrichment of CgCrzA-bound DNA fragments under CFW conditions (Fig. 4A). Analysis of the ChIP-seq data identified 3,894 peaks as potential binding sites of the CgCrzA target genes (Fig. 4B). Using multiple MEME tools, we identified a 12-bp binding region as potential CgCrzA-bound motifs (Fig. 4C). Binding site analysis of these peaks reveal their localization in intergenic regions (17.21%), upstream 2-kb regions (2.63%), downstream 300 bp regions (0.19%), and intron/exon regions (0.91%) (Fig. 4D). Genome-wide annotation indicated that the 3,894 overlapping peaks corresponded to 2,944 genes distributed evenly throughout the genome (Fig. 4E). Gene Ontology analysis revealed that these 2,944 target genes were

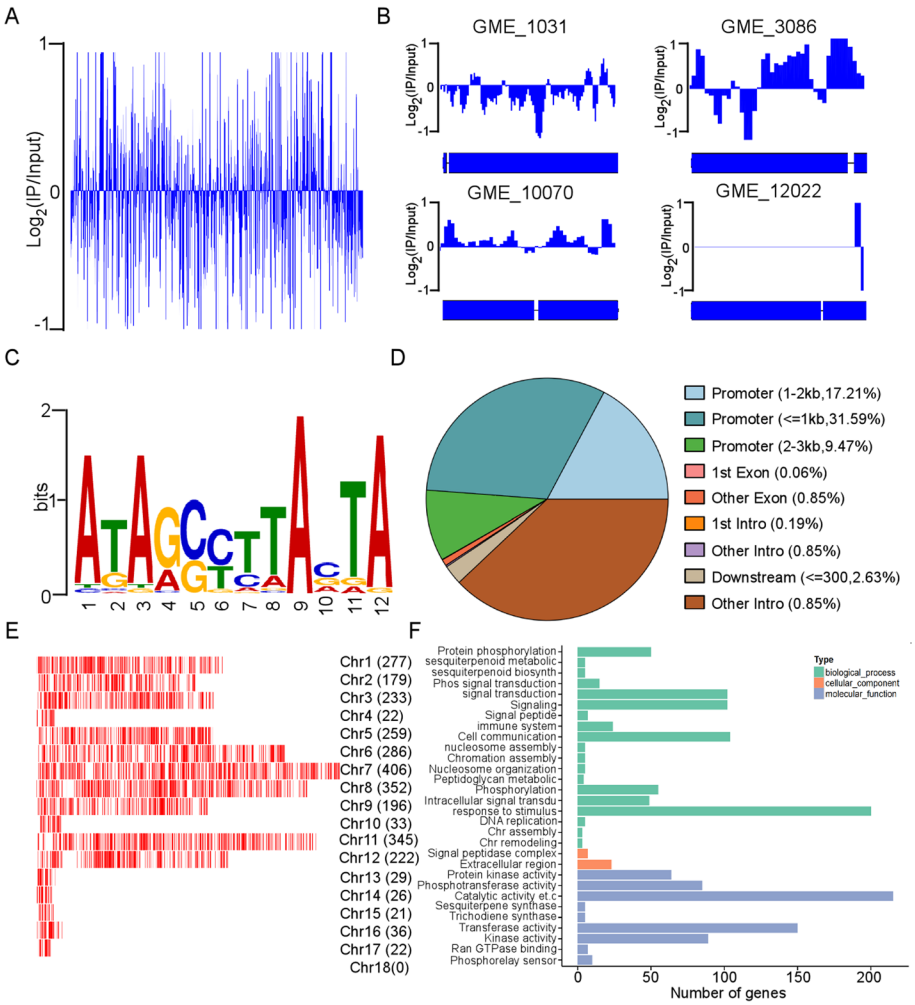

Fig. 4 Identification of direct transcriptional targets of CgCrzA under CFW conditions through Genome-wide ChIP-seq analysis. **A** Genome-scale view of ChIP-seq data represented as $\log_2$ (IP_{RPKM}/$Input_{RPKM}$) signals calculated for each 50 bp. Enriched ChIP signals above the horizontal blue line ($\log_2 IP_{RPKM}/Input_{RPKM} = 0$) indicate significant binding compared to the input control. **B** Snapshot ChIP of signals for genes identified in (**A**). **C** Most likely DNA motif bound by CgCrzA, identified using MEME tools. **D** Distribution of peaks among different gene features in *C. gloeosporioides*. **E** Genome-wide distribution of putative CgCrzA target genes. **F** Gene Ontology categorization of the putative CgCrzA target genes

involved in diverse biological processes and molecular functions, with a notable representation in response to stimulus and catalytic processes (Fig. 4F).

CgCrzA targets the chitin synthase genes *CgCHS5* and *CgCHS6* under CFW conditions

Through screening of the target genes for the transcription factor CgCrzA using ChIP-seq (Additional file 2: Table 1), the chitin synthase genes *CgCHS5* and *CgCHS6* were identified as potential targets under CFW conditions. Analysis of the expression of *CgCHS5* and *CgCHS6* in the hyphae (HY) and conidia (CO) using quantitative RT-PCR revealed significant upregulation upon CFW treatment in the wild-type, whereas their transcription remained basal in the Δ*CgcrzA* mutant (Fig. 5A, B).

DNA retardation assays were performed by incubating purified CgCrzA^{S280D} protein with DNA fragments containing the promoter sequences of *CgCHS5* and *CgCHS6*. Retardation of the DNA fragments was observed upon exposed to CgCrzA^{S280D} protein, whereas no retardation was evident with GST proteins (Fig. 5C). Moreover, the degree of retardation

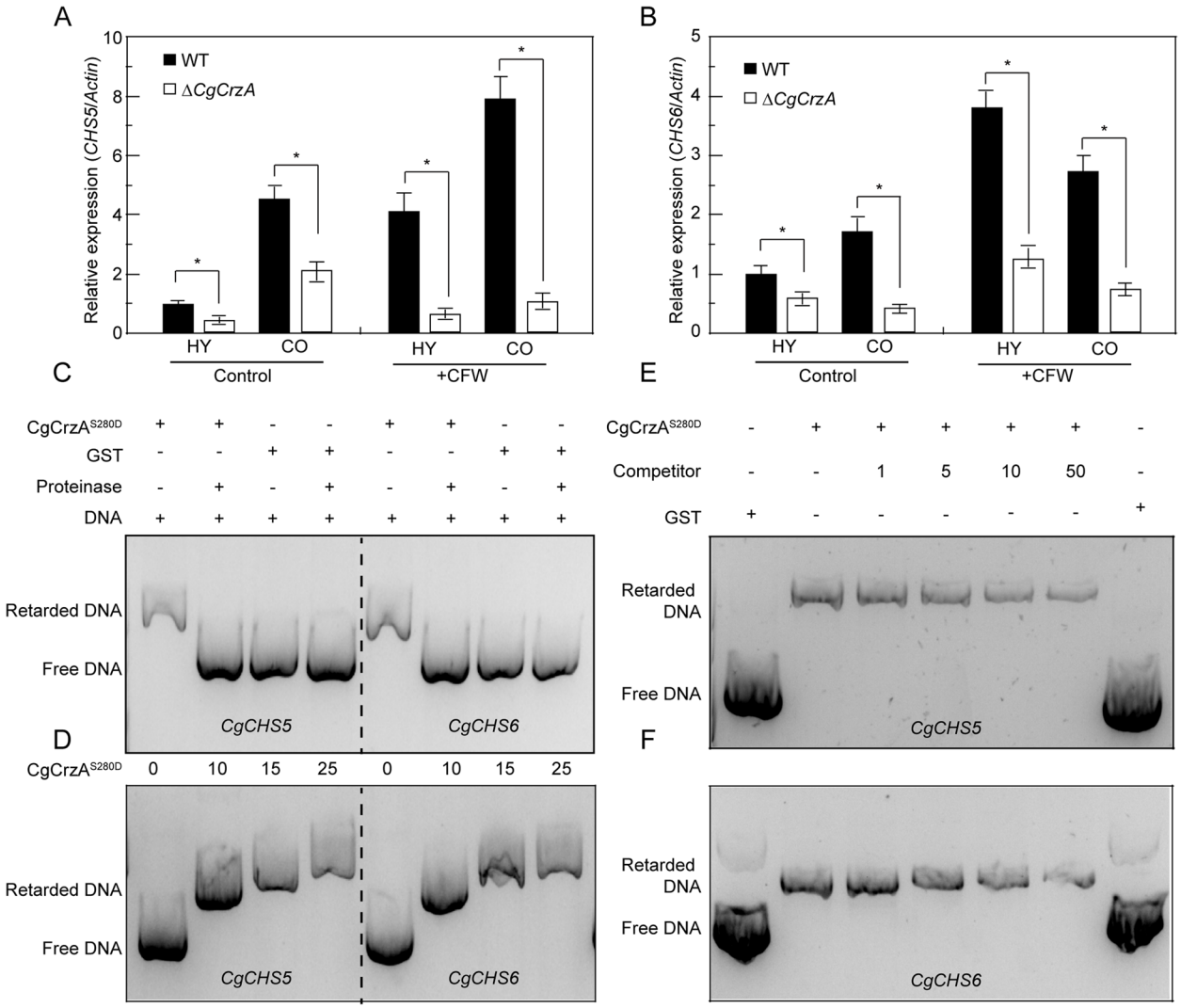

Fig. 5 Binding of CgCrzA to the promoter regions of *CgCHS5* and *CgCHS6*. **A**, **B** Quantitative RT-PCR analysis of *CgCHS5/6* expression in the Δ*CgcrzA* mutant and wild-type in response to CFW. HY and CO indicates hypha and conidia, respectively. Error bars represent standard deviation. Asterisks indicate a significant difference at $P < 0.01$. **C** and **D** Electrophoretic Mobility Shift Assay (EMSA) demonstrating the binding of CgCrzA^{S280D} protein to the putative promoter sequences of CgCHS5 (**C**) and CgCHS6 (**D**). The band shift of the promoter with increasing concentration of CgCrzA^{S280D} protein. GST indicates glutathione S-transferase tag protein. **E** and **F** Incubation of the Alex660-labelled full-length promoter DNA in the absence (leftmost lane) or presence (second to the sixth lane) of purified CgCrzA^{S280D} and GST proteins (rightmost lane). Unlabelled DNA was added as a binding competitor, with increasing amounts in the third to sixth lanes

increased with increasing amounts of CgCrzA^{S280D} protein (Fig. 5D). To further validate these findings, electrophoretic mobility shift assays (EMSA) were conducted. The results demonstrated that purified CgCrzA^{S280D} protein bound to the Alex660-labelled promoter DNA fragments of *CgCHS5* and *CgCHS6*, with binding ability decreased as the concentration of unlabeled competitor DNA fragment increased (Fig. 5E, F).

The target genes *CgCHS5* and *CgCHS6* are involved in pathogenicity and CWI

Phenotypic analysis of *CgCHS5* and *CgCHS6* deletion mutants generated using a gene replacement strategy (Additional file 1, Fig. S5) revealed significant defects in vegetative growth and conidiation for both Δ*Cgchs5* and Δ*Cgchs6* mutants (Fig. 6A-C). Pathogenicity tests showed that the Δ*Cgchs5* and Δ*Cgchs6* mutants typically displayed restricted lesions, whereas the wild-type and complemented strains exhibited coalescent lesions (Fig. 6D). Δ*Cgchs5* and Δ*Cgchs6* mutants showed increased susceptibility to the cell wall inhibitors CFW and Congo Red (Additional file 1, Fig. S6). Compared to the wild-type, protoplast release from Δ*Cgchs5* and Δ*Cgchs6* mutants was significantly accelerated when treated with cell wall-degrading enzymes (Fig. 6E). These mutants showed decreased chitin content in the mycelia compared to the wild-type (Fig. 6F).

Discussion

MAPK, G-protein, and calcium-mediated signal transduction pathways have been implicated in various aspects of the development and pathogenicity in several plant pathogenic fungi. The calcium signal relay mediated by the transcription factor CgCrzA was characterised in *C. gloeosporioides* [21]. The Δ*CgcrzA* mutant displayed

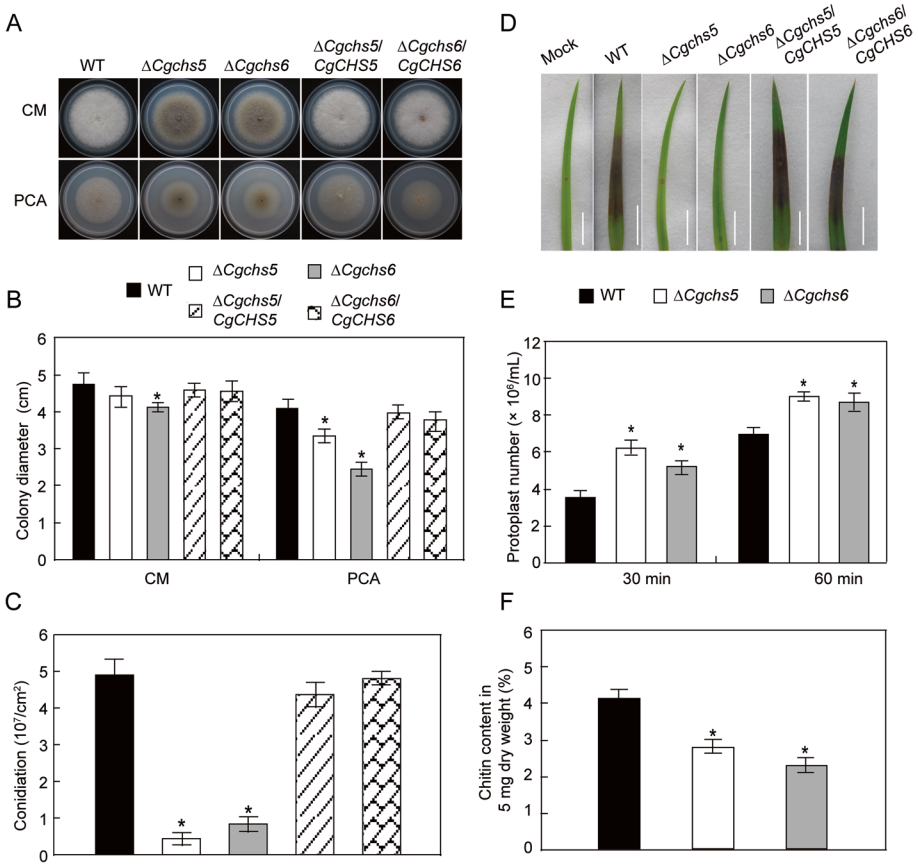

Fig. 6 Impact of CgChs5 and CgChs6 on vegetative growth, asexual development, and virulence. **A** Colonies of the wild-type (WT), Δ*Cgchs5*, Δ*Cgchs6*, Δ*Cgchs5*/*CgCHS5*, and Δ*Cgchs6*/*CgCHS6* strains on CM and PCA plates at 28°C for 4 days in the dark. **B** Statistical analysis of the colony diameter for the indicated strains in (**A**). **C** Quantification of conidia produced by the indicated strains. **D** Lesions developed on wounded leaves of *C. lanceolata* inoculated with conidial suspensions of the WT, Δ*Cgchs5*, Δ*Cgchs6*, Δ*Cgchs5*/*CgCHS5*, and Δ*Cgchs6*/*CgCHS6* strains for 5 days. **E** Protoplast release from the WT, Δ*Cgchs5*, Δ*Cgchs6* strains after treatment with cell wall-degrading enzymes for 30 and 60 min at 30°C. **F** Measurement of mycelial chitin content of the WT, Δ*Cgchs5*, and Δ*Cgchs6* strains. Error bars represent standard deviation. Asterisks indicate a significant difference at $P < 0.01$

similar phenotypes defects when exposed to Ca^{2+} or the cell wall inhibitor CFW. Additionally, our previous work discovered that CgCrzA plays a role in plant infection by regulating appressorium and invasive hyphae [2]. Here, to reveal the mechanism of CgCrzA regulating cell wall integrity and pathogenicity in C. *gloeosporioides*, we employed a genome-wide approach to identify the direct downstream targets of CgCrzA under CFW stress through ChIP-chip analysis. Our study reveals an additional role for CgCrzA in responding to CFW-induced stress and elucidates the underlying mechanism in *C. gloeosporioides*. Our findings provide evidence that exogenous CFW induces phosphorylation of CgCrzA at Ser280, a process dependent on the MAPK CgMkk1. This phosphorylation triggers the translocation of CgCrzA from the cytoplasm into the nucleus. Subsequently, phosphorylated CgCrzA preferentially binds to the promoter sites of chitin synthase genes *CgChs5* and *CgChs6*, thereby up-regulating their expression. This reinforces cell wall integrity (CWI) and protects fungal cells against cell wall stress in *C. gloeosporioides*.

Pathogenic fungal mitogen-activated protein kinase (MAPK) cascades, including CgMkk1, play crucial roles in the development of invasive structures and responses to variousstresses [7, 10, 22]. MAPK cascades (Mck1-Mkk1-Mps1) by phosphorylated downstream target genes is required for maintenance of CWI, stresses response and pathogenicity in phtyopathogen fungi, including *M. oryzea*, *F. oxysporum* and others [7, 23]. Our previous studies revealed that the MAPK CgMkk1 is required for development, CWI, and infection morphogenesis in *C. gloeosporioides* [10], yet the underlying mechanism remained unclear. In this study, we identified an interaction between CgMkk1 and the transcription factor CgCrzA. Deletion of CgCrzA led to the similar phonotype defects of CWI and pathogenicity to the Δ*Cgmkk1* mutant (Fig. S1). Further analysis revealed that CgMkk1 phosphorylates CgCrzA and promotes its translocation from the cytoplasm to the nucleus. Mass spectrometry and Mn^{2+}-Phos-tag assays provided additional evidence supporting CgMkk1-mediated phosphorylation of CgCrzA at Ser280. We expressed the phosphomimetic mutant $CgCrzA^{S280D}$ in the Δ*Cgmkk1* mutant, resulting in enhanced resistance to cell wall inhibitors and increased pathogenicity. Conversely, the phosphor-dead mutant $CgCrzA^{S280A}$ exhibited defects in CWI and pathogenicity similar to the Δ*CgcrzA* mutant. These findings underscore the critical role of CgCrzA phosphorylation at Ser280, dependent on CgMkk1, in maintaining CWI and facilitating pathogenicity in *C. gloeosporioides*. Notably, this study is the first report of Mkk1-mediated phosphorylation of transcription factor CrzA in filamentous fungi.

It is increasingly evident that transcription factors (TFs) play a crucial role in plant-pathogenic fungi [24]. While TFs primarily function by binding to specific DNA sequences, their activity can be modulated by posttranslational modifications and subcellular localization [25, 26]. For instance, phosphorylation regulates the activity of the transcription factor CreA in the *Aspergillus nidulans*. Upon increased phosphorylation, CreA translocates into the nucleus and subsequently binds to target genes, thereby controlling their expression [27]. Similarly, in our study, we found that CgMkk1-mediated phosphorylation of CgCrzA facilitates its translocation into the nucleus. Furthermore, we observed that under CFW stress conditions, CgCrzA failed to translocate into the nucleus in the Δ*CgMkk1* mutant, while in the wild type, CgCrzA completely translocated into the nucleus from the cytoplasm with CFW treatment (Fig. 2). These results suggest that phosphorylation of CgCrzA by the MAPK kinase CgMkk1 is responsible for its nuclear translocation in response to the cell wall inhibitor CFW.

Chitin, an essential component of the cell wall, plays a vital role in maintaining cell wall integrity and protecting fungal cells from various stresses [1]. It is a linear polymer composed of N-acetylglucosamine (GlcNAc) monomers linked by β-1,4-glycosidic bonds [28]. Biosynthesis of chitin is catalyzed by chitin synthases (Chs), which polymerize GlcNAc into chitin [29–31]. While *Saccharomyces cerevisiae* possesses three chitin synthases, some filamentous fungi utilize more than seven chitin synthases for chitin biosynthesis [29, 30]. Chs in pathogenic fungi, such as *M. oryzae*, *A. fumigatus*, *B. cinerea*, and *F. graminearum*, are classified into seven groups based on their sequence similarities and functional characteristics [14, 32, 33]. These Chs groups have been shown to have diverse roles in vegetative growth, conidiation, appressorium development, and pathogenesis. For instance, in *M. oryzae*, Chs1 is essential for conidiogenesis [14]. While deletion of the *CHS6* results in reduced vegetative growth, decreased conidiation, and impaired invasive growth [14]. The mutant Δ*Mochs7* shows defects in appressorium development and invasive growth, highlighting the importance of Chs7 in these processes [14]. Here, CgChs5 and CgChs6 belong to class V and VI chitin synthases, respectively, identified as downstream targets of the TF CgCrzA. Both CgChs5 and CgChs6 play essential roles in vegetative growth and plant infection by regulate synthesis of chitin and CWI in *C. gloeosporioides* (Fig. 6). Additionally, since chitin is absent in plant and mammals, chitin synthases might be a promising fungicidal target for the control of fungal pathogens [34, 35]. Considering the extreme important of CgChs5 and CgChs6, they can become ideal target for new fungicides.

In *C. gloeosporioides*, similar to their counterparts in other filamentous ascomycetes, *CgCHS5* and *CgCHS6* are positioned adjacently in a head-to-head arrangement in the genome. This genomic arrangement suggests that *CHS5* and *CHS6* may share common regulatory elements in their promoter regions. Studies have reported that phosphorylated transcription factors, such as OsIPA1 and TaCBF1 in plants, preferentially bind to the promoter regions to enhance the expression of their target genes [36, 37]. Similarly, in *M. oryzae*, the conserved MAPK MoPmk1 phosphorylates the transcription factor Hox7, which regulates target genes involved in appressorium development, including turgor generation and melanin biosynthesis [38]. The phosphorylation CgCrzA upregulated expression levels of *CHS5* and *CHS6*, which strengthens cell wall integrity, enabling the phytopathogen to withstand the action of cell wall-degrading enzymes. Thus, we speculate that the compromised virulence observed in the mutants Δ*Cgchs5* and Δ*Cgchs6* could be attributed, at least in part, to the defect in cell wall integrity. These findings provide further insights into the regulatory mechanisms of *CHS5* and *CHS6* in pathogenic fungi.

Conclusions

In our study, we observed similar defects in cell wall integrity (CWI) and plant infection when deleting *CgMKK1*, *CgCRZA*, and *CgCHS5/6* in *C. gloeosporioides*. Additionally, we uncovered a novel regulatory mechanism of CgMkk1-CgCrzA-CgChs5/6, which enables *C. gloeosporioides* to respond to the cell wall inhibitor CFW and facilitate infectious growth. The proposed regulatory mechanism is illustrated in Fig. 7 of our study. In summary, our findings uncover a previously unknown regulatory mechanism that allows *C. gloeosporioides* to respond to CFW stress. Furthermore, our studies uncover a previously unknown regulatory and their functions provide valuable insights that could aid in the development of novel strategies for controlling anthracnose disease.

Methods

Fungal strains and culture conditions

The *C. gloeosporioides* SMCG1#C was used as the wild-type (WT) in the present study. The Δ*CgcrzA* and Δ*Cgmkk1* mutants, and their complemented strains were previously generated [10, 21]. The other mutants were generated in this study. All strains were maintained on complete medium (CM)

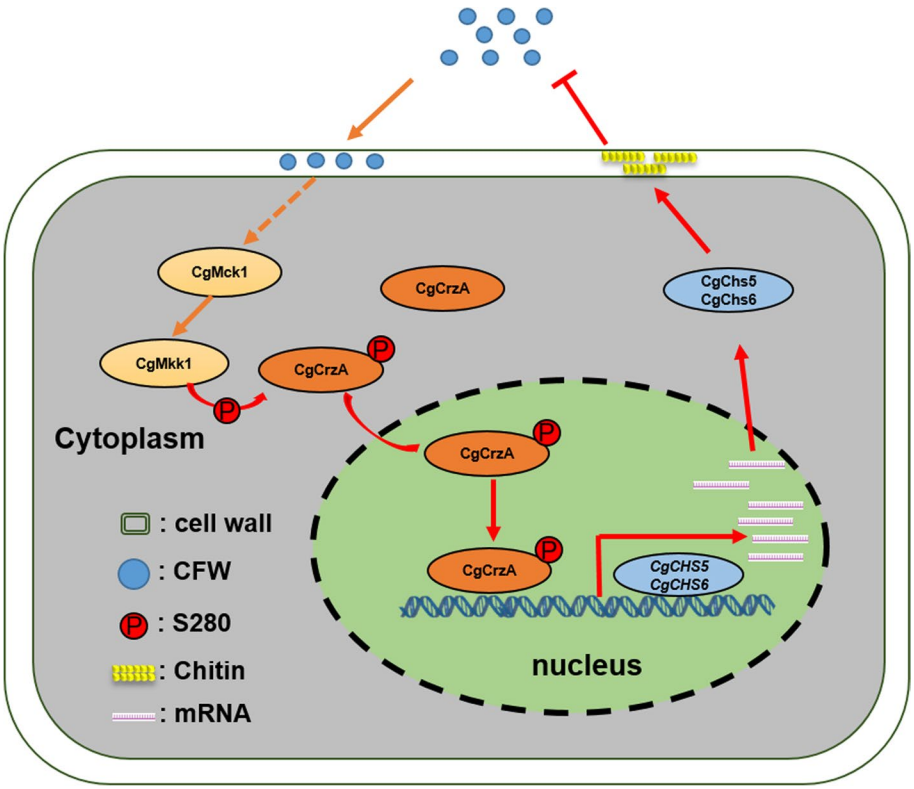

Fig. 7 A proposed model illustrating the involvement of CgCMkk1, CgCrzA, and CgChs5/6 in response to CFW stress in *C. gloeosporioides*. Under CFW conditions, CgMkk1 phosphorylates CgCrzA at Ser280. This phosphorylation event leads to the translocation of CgCrzA from the cytoplasm into the nucleus. In the nucleus, phosphorylated CgCrzA preferentially binds to the promoter regions of *CgCHS5/6*, resulting in their expression. The expression of *CgCHS5/6* promotes the biosynthesis of chitin, which is crucial for maintaining CWI. This, in turn, facilitates infectious growth and contributes to the survival of the pathogen

agar plates at 28°C [21]. Mycelia for DNA and RNA extraction were cultured in liquid CM, as described previously [21]. Growth assays were performed by incubating the indicated strains in CM and potato dextrose agar (PDA) plates at 28°C, for 4 days [21]. For cell wall stress resistance assays, strains were cultured on CM supplemented with calcofluor white (CFW) in the dark and maintained at 28°C for 4 days.

Gene deletion and complementation

Gene deletion mutants were generated using a one-step gene replacement strategy [2]. The *CgCHS5/6* gene deletion constructs were generated by amplification 1.0 kb upstream and downstream flanking sequences from SMCG1#C genomic DNA using polymerase chain reaction (PCR). Subsequently, PCR products, along with the hygromycin phosphotransferase cassette, were amplified using split-marker PCR [21]. The resulting 3.4 kb fragments were transformed into protoplasts of the WT strain, as described previously [21]. To obtain complemented strains, a fragment containing the entire *CgCHS5/6* gene and its native promoter regions (upstream 1.5 kb) were amplified by PCR using the WT genomic DNA as a template, followed by insertion into pYF11 to complement the mutant strains.

Yeast two-hybrid (Y2H) and co-immunoprecipitation (co-IP) assays

The full-length cDNAs of CgCrzA and CgMkk1 were cloned into pGBKT7 and pGADT7, respectively, to ascertain the in vitro interactions between these two proteins. The sequences were validated, and constructs were then transformed together into the yeast strain AH109, as previously described [39].

For in vivo interactions, CgCrzA-GFP and CgMkk1-S fusion constructs were prepared via yeast homologous recombination transformation and co-transformed into protoplasts of the WT. Total proteins were extracted from the transformants and incubated with anti-green fluorescent protein (GFP) beads. The proteins bound to the beads were eluted and subjected to western blot with anti-GFP and anti-S antibodies, as previously described [40].

Staining and confocal microscopy

To assess the impact of CFW on the translocation of CgCrzA, hyphae from the strain co-expressing CgCrzA-GFP and H1-RFP were pre-treated with CFW for 60 and 120 min, and then observed under a confocal fluorescence microscope (LSM880, 40×oil; Zeiss). Vegetative hyphae cultured in liquid CM for 16 h were stained with CFW to examine chitin, following established protocols [6].

Pathogenicity assays

Virulence tests were conducted by inoculating 10 μL of conidia suspensions (1×10^5 spores mL^{-1}) on unwounded leaves of *C. lanceolata* (Lambert) Hooker. Inoculated leaves were kept in a moist chamber maintained at 25 °C with 90% humidity and darkness for the initial 24 h, followed by exposure to a 16-h light/ 8-h dark cycle [21]. Disease lesions were evaluated and photographed 5 days post-inoculation.

Protoplast-release and chitin content assays

Protoplast-release experiment was conducted by culturing mycelia in CM for 16 h, followed by collection, washing, and resuspension in a lysing enzyme solution [21]. The protoplast-release was counted at 30 and 60 min, respectively, under a light microscope.

To determine the chitin content, mycelia of the indicated strain were freeze-dried and finely ground. Five mg of mycelia were treated with 1 mL of 6% KOH at 80 °C for 1.5 h. The mixture was centrifuged at 12,000 rpm for 10 min, and the precipitates were washed three times with phosphate-buffered saline. The precipitates were then suspended in 0.5 mL of McIlvaine's buffer. An aliquot of 100 μL of chitinase (13 units) was added and the mixture was incubated at 37 °C for 16 h. Then, 100 μL of 0.27 M sodium borate were mixed with the sample and boiled for 10 min. The sample was mixed with 1 mL of diluted Ehrlich's reagent and further incubated at 37 °C for 20 min. One mL of the sample was transferred to a 2.5 mL plastic cuvette (Greiner, Frickenhausen, Germany) and the absorbance was measured at a wavelength of 585 nm.

Phosphorylation assays

For in vivo phosphorylation analysis, CgCrzA-GFP fusion constructs were introduced into the WT and Δ*Cgmkk1* strains, respectively. Fresh mycelia (150 to 200 mg) were finely ground and added to 1 mL extraction buffer [150 mM NaCl, 0.5 mM EDTA, 10 mM Tris-HCl (pH 7.5), 0.5% NP40], supplemented with 1 mM PMSF and 10 μL of a protease inhibitor cocktail (Sigma). The sample was then incubated at 37 °C for 1 h, following the addition of 2.5 U/mL alkaline phosphatase (Sigma) and 10 μL of phosphatase-treated cell lysates. The mixture was resolved on 8% sodium dodecyl sulfate-polyacrylamide gels, prepared with 50 μM acrylamide-dependent Phos-tag and 100 μm $MnCl_2$, as previously detailed [41].

His-CgCrzA and GST-CgMkk1 were expressed in *E. coli* strain *BL21* (DE3) and purified using an established procedure [41]. Subsequently, 2 mg of CgMkk1 protein was mixed with CgCrzA in a kinase reaction buffer (consisting of 100 mM phosphate-buffered saline, 1 mM ascorbic acid at pH 7.5, and 10 mM $MgCl_2$), supplemented with 50 mM ATP. The reaction was incubated at 25°C for 1 h, followed by termination with 10-fold cold acetone. Protein phosphorylation in vitro was analysed

using the The Pro-Q™ Diamond Phosphorylation Gel Stain with the Rapid Fluorescence Detection in Tube (FDIT) method [42].

Mass spectrometric analysis

To identify the phosphorylation sites of CgCrzA, total proteins were extracted from the WT/CgCrzA-GFP and Δ*Cgmkk1*/CgCrzA-GFP transformants, and subjected to purification steps described previously. Purified proteins were separated via 10% sodium dodecyl sulfate-polyacrylamide gel electrophoresis (SDS-PAGE). Gel bands corresponding to CgCrzA were excised and analyzed using a Thermo Q-Exactive high-resolution mass spectrometer (Thermo Scientific, Waltham, MA). Phosphorylated sites were identified by MS/MS spectra data with Mascot Distiller (Matrix Science; version 2.4).

Quantitative RT-PCR analysis

Total RNA extraction was carried out using an RNA extraction kit (Invitrogen, USA). Subsequent cDNA synthesis was performed using M-MLV reverse transcriptase (Vazyme Biotech, Nanjing, China) according to the manufacturer's instructions. The resulting cDNA was employed for quantitative PCR on a Real-time PCR system with ChamQ SYBR® qPCR Mix (Q311-02, Vazyme Biotech). Normalization and comparison of mean cycle threshold (Ct) values were conducted as described in a previous study [12].

Electrophoretic mobility shift assay

The cDNA of $CgCrzA^{S280D}$ was cloned into the pET-32a vector to heterogeneously express the His-tagged $CgCrzA^{S280D}$ protein. Expression of the $CgCrzA^{S280D}$ protein was carried out in *E. coli* BL21-Codonplus (DE3) cells and purified using Ni-NTA agarose (Sigma) according to the manufacturer's instructions. A DNA fragment (2.0-kb upstream flanking sequences) of the *CgCHS5/6* gene promoter was amplified by PCR with the appropriate primers (as listed in Additional file 3: Table 2). The purified $CgCrzA^{S280D}$ protein was then mixed with the amplified promoter fragment, and the mixture was incubated at 25°C for 20 min. Results were separated using agarose gel electrophoresis and visualized directly using an Odyssey® scanner (LI-COR) with excitation at 700 nm wavelength, as described in a study by Wang et al. [43].

Statistical analysis

Each result is presented as mean ± standard deviation of at least three independent replicates. Significant differences between treatments were determined using a one-way analysis of variance (ANOVA) with SPSS 2.0. If the ANOVA result was significant at $p < 0.01$, a post-hoc F-test was performed to compare the data among different treatments.

Abbreviations

CWI	Cell wall integrity
CFW	Calcofluor white
CR	Congo Red
PI	Phosphatase inhibitors
CHS genes	Chitin synthase genes
CrzA	Calcineurin-regulated zinc-finger factor A
MAPK	Mitogen-activated protein kinase
SDS-PAGE	Sodium dodecyl sulfate-Polyacrylamide gel electrophoresis
GFP	Green fluorescent protein
Y2H	Yeast two-hybrid
IP	Immunoprecipitation
CBB	Coomassie Brilliant Blue
LC-MS/MS analysis	Liquid Chromatography-Mass Spectrometry
ChIP-seq	Chromatin immunoprecipitation followed by sequencing analysis
HY	Hyphae
CO	Conidia
EMSA	Electrophoretic mobility shift assays

Supplementary Information

The online version contains supplementary material available at https://doi.org/10.1186/s12915-024-01978-y.

Additional file 1: Fig. S1. Impact of CgMkk1 on development and virulence. Fig. S2. Deficiency in cell wall integrity observed in the Δ*Cgmkk1* mutant. Fig. S3. Role of CgMkk1 in response to cell wall stressors. Fig. S4. Roles of CgCrzA phosphorylation at Ser280 in vegetative growth. Fig. S5. Targeted deletion of *CgCHS5* and *CgCHS6* in *C. gloeosporioides*. Fig. S6. Role of CgChs5 and CgChs6 in response to stresses of cell wall inhibitors.

Additional file 2: Table 1. The target genes for the transcription factor CgCrzA by ChIP-seq.

Additional file 3: Table 2. Primers used in this study.

Acknowledgements

We thank Zhengguagn Zhang at Nanjing Agricultural University for the pYF11 plasmids; Wenxian Sun at Jilin Agricultural University for valuable comments. Sheng Zhu at Nanjing forestry University for the support in database analysis.

Research on plants

This research complies with the relevant institutional, national, and international guidelines and legislation on conducting research on plants.

Authors' contributions

JYY, BL and LH designed research; BL, TYP, PW, MSS, JYY performed experiments; BL and LH contributed new reagents/analytical tools; KTK, JYY, HS, ZJ and HYL analyzed data; and BL, JYY and LH wrote the manuscript. All authors read and approved the final manuscript. The authors declare no competing financial interests.

Funding

This study was supported by the National Science Foundation of China (Grant No: 32101530; 31870631; 32371888), the National Key R & D Program of China (2017YFD0600102), the Foundation of Key Technology Research Project of Henan Province (Grant No: 222102110031), China Postdoctoral Science Foundation (Grant No:2022M712886), and Priority Academic Program Development of Jiangsu Higher Education Institutions (PAPD).

Availability of data and materials

All data generated or analyzed during this study are included in this published article, its supplementary information files and publicly available repositories. The ChIP-seq database is free available at https://doi.org/10.6084/m9.figshare.26503291 [44]. The phosphorylation sites of CgCrzA were identified by LC-MS/MS is free available at https://doi.org/10.6084/m9.figshare.26500237.v1 [45].

Declarations

Ethics approval and consent to participate
Not applicable.

Consent for publication
Not applicable.

Competing interests
The authors declare that they have no competing interests.

Received: 22 January 2024 Accepted: 12 August 2024
Published online: 26 August 2024

References

1. Gow NAR, Latge JP, Munro CA. The fungal cell wall: structure, biosynthesis, and function. Microbiol Spect. 2017;5(3):10. https://doi.org/10.1128/microbiolspec.FUNK-0035-2016.
2. Feng WZ, Yin ZY, Wu HW, Liu P, Liu XY, Liu MX, et al. Balancing of the mitotic exit network and cell wall integrity signaling governs the development and pathogenicity in *Magnaporthe oryzae*. PLoS Pathog. 2021;17(1):e1009080. https://doi.org/10.1371/journal.ppat.1009080.
3. Hofte H, Voxeur A. Plant cell walls. Curr Biol. 2017;27(17):865–70. https://doi.org/10.1016/j.cub.2017.05.025.
4. Naseer S, Lee Y, Lapierre C, Franke R, Nawrath C, Geldner N. Casparian strip diffusion barrier in *Arabidopsis* is made of a lignin polymer without suberin. Proc Natl Acad Sci U S A. 2012;109(25):10101–6. https://doi.org/10.1073/pnas.1205726109.
5. Vaahtera L, Schulz J, Hamann T. Cell wall integrity maintenance during plant development and interaction with the environment. Nat Plants. 2019;5(9):924–32. https://doi.org/10.1038/s41477-019-0502-0.
6. Yang C, Yu Y, Huang J, Meng F, Pang J, Zhao Q, et al. Binding of the *Magnaporthe oryzae* chitinase MoChia1 by a rice tetratricopeptide repeat protein allows free chitin to trigger immune responses. Plant Cell. 2019;31(1):172–88. https://doi.org/10.1105/tpc.18.00382.
7. Yin ZY, Tang W, Wang JZ, Liu XY, Yang LN, Gao CY, et al. Phosphodiesterase MoPdeH targets MoMck1 of the conserved mitogen-activated protein (MAP) kinase signalling pathway to regulate cell wall integrity in rice blast fungus *Magnaporthe oryzae*. Mol Plant Pathol. 2016;17(5):654–68. https://doi.org/10.1111/mpp.12317.
8. Irie K, Takase M, Lee KS, Levin DE, Araki H, Matsumoto K, Oshima Y. Mkk1 and Mkk2, which encode *Saccharomy cescerevisiae* mitogen-activated protein kinase-kinase homologs, function in the pathway mediated by protein-kinase-C. Mol Cell Biol. 1993;13(5):3076–83. https://doi.org/10.1128/mcb.13.5.3076-3083.1993.
9. Xu JR, Staiger CJ, Hamer JE. Inactivation of the mitogen-activated protein kinase Mps1 from the rice blast fungus prevents penetration of host cells but allows activation of plant defense responses. Proc Natl Acad Sci U S A. 1998;95(21):12713–8. https://doi.org/10.1073/pnas.95.21.12713.
10. Fang YL, Xia LM, Wang P, Zhu LH, Ye JR, Huang L. The MAPKKK CgMck1 is required for cell wall integrity, appressorium development, and pathogenicity in *Colletotrichum gloeosporioides*. Genes. 2019;10(10):819. https://doi.org/10.3390/genes9110543.
11. Jeon J, Goh J, Yoo S, Chi MH, Choi J, Rho HS, et al. A putative MAP kinase kinase kinase, MCK1, is required for cell wall integrity and pathogenicity of the rice blast fungus, *Magnaporthe oryzae*. Mol Plant Microbe Interact. 2008;21(5):525–34. https://doi.org/10.1094/MPMI-21-5-0525.
12. Yin ZY, Feng WZ, Chen C, Xu JY, Li Y, Yang LN, et al. Shedding light on autophagy coordinating with cell wall integrity signaling to govern pathogenicity of *Magnaporthe oryzae*. Autophagy. 2020;16(5):900–16. https://doi.org/10.1080/15548627.2019.1644075.
13. Lenardon MD, Munro CA, Gow NA. Chitin synthesis and fungal pathogenesis. Curr Opin Microbiol. 2010;13(4):416–23. https://doi.org/10.1016/j.mib.2010.05.002.
14. Kong LA, Yang J, Li GT, Qi LL, Zhang YJ, Wang CF, et al. Different chitin synthase genes are required for various developmental and plant infection processes in the rice blast fungus *Magnaporthe oryzae*. PLoS Pathog. 2012;8(2):e1002526. https://doi.org/10.1371/journal.ppat.1002526.
15. Sanchez-Leon E, Verdin J, Freitag M, Roberson RW, Bartnicki-Garcia S, Riquelme M. Traffic of chitin synthase 1 (*CHS*-1) to the Spitzenkorper and developing septa in hyphae of *Neurospora crassa*: actin dependence and evidence of distinct microvesicle populations. Eukaryot Cell. 2011;10(5):683–95. https://doi.org/10.1128/EC.00280-10.
16. Takeshita N, Yamashita S, Ohta A, Horiuchi H. *Aspergillus nidulans* class V and VI chitin synthases CsmA and CsmB, each with a myosin motor-like domain, perform compensatory functions that are essential for hyphal tip growth. Mol Microbiol. 2006;59(5):1380–94. https://doi.org/10.1111/j.1365-2958.2006.05030.x.
17. Weber I, Assmann D, Thines E, Steinberg G. Polar localizing class V myosin chitin synthases are essential during early plant infection in the plant pathogenic fungus *Ustilago maydis*. Plant Cell. 2006;18(1):225–42. https://doi.org/10.1105/tpc.105.037341.
18. Kim S, Hu J, Oh Y, Park J, Choi J, Lee YH, et al. Combining ChIP-chip and expression profiling to model the *MoCRZA* mediated circuit for Ca^{2+}/calcineurin signaling in the rice blast fungus. PLoS Pathog. 2010;6(5):e1000909. https://doi.org/10.1371/journal.ppat.1000909.
19. Stathopoulos AM, Cyert MS. Calcineurin acts through the CRZ1/TCN1-encoded transcription factor to regulate gene expression in yeast. Genes Dev. 1997;11(24):3432–44. https://doi.org/10.1101/gad.11.24.3432.
20. Dubey AK, Barad S, Luria N, Kumar D, Espeso EA, Prusky DB. Cation-stress-responsive transcription factors SltA and CrzA regulate morphogenetic processes and pathogenicity of *Colletotrichum gloeosporioides*. PLoS One. 2016;11(12):e0168561. https://doi.org/10.1371/journal.pone.0168561.
21. Wang P, Li B, Pan YT, Zhang YZ, Li DW, Huang L. Calcineurin-responsive transcription factor CgCrzA is required for cell wall integrity and infection-related morphogenesis in *Colletotrichum gloeosporioides*. Plant Pathol J. 2020;36(5):385–97. https://doi.org/10.5423/PPJ.OA.04.2020.0071.
22. Xu JR. Map kinases in fungal pathogens. Fungal Genet Biol. 2000;31(3):137–52. https://doi.org/10.1006/fgbi.2000.1237.
23. Ding Z, Li M, Sun F, Xi P, Sun L, Zhang L, Jiang Z. Mitogen-activated protein kinases are associated with the regulation of physiological traits and virulence in *Fusarium oxysporum* f. sp. cubense. PLoS One. 2015;10(4):e0122634. https://doi.org/10.1371/journal.pone.0122634.
24. John E, Singh KB, Oliver RP, Tan KC. Transcription factor control of virulence in phytopathogenic fungi. Mol Plant Pathol. 2021;22(7):858–81. https://doi.org/10.1111/mpp.13056.
25. Levo M, Avnit-Sagi T, Lotan-Pompan M, Kalma Y, Weinberger A, Yakhini Z, Segal E. Systematic investigation of transcription factor activity in the context of chromatin using massively parallel binding and expression assays. Mol Cell. 2017;65(4):604–17. https://doi.org/10.1016/j.molcel.2017.01.007.
26. Sri Theivakadadcham VS, Bergey BG, Rosonina E. Sumoylation of DNA-bound transcription factor Sko1 prevents its association with nontarget promoters. PLoS Genet. 2019;15(2):e1007991. https://doi.org/10.1371/journal.pgen.1007991.
27. De Assis LJ, Silva LP, Bayram O, Dowling P, Kniemeyer O, Krüger T, et al. Carbon catabolite repression in filamentous fungi is regulated by phosphorylation of the transcription factor CreA. mBio. 2021;12(1):e03146-20. https://doi.org/10.1128/mBio.03146-20.
28. Roncero C. The genetic complexity of chitin synthesis in fungi. Curr Genet. 2002;41(6):367–78. https://doi.org/10.1007/s00294-002-0318-7.
29. Bowen AR, Chen-Wu JL, Momany M, Young R, Szaniszlo PJ, Robbins PW. Classification of fungal chitin synthases. Proc Natl Acad Sci U S A. 1992;89(2):519–23. https://doi.org/10.1073/pnas.89.2.519.
30. Morozov AA, Likhoshway YV. Evolutionary history of the chitin synthases of eukaryotes. Glycobiology. 2016;26(6):635–9. https://doi.org/10.1093/glycob/cww018.
31. Lenardon MD, Whitton RK, Munro CA, Marshall D, Gow NA. Individual chitin synthase enzymes synthesize microfibrils of differing structure at specific locations in the *Candida albicans* cell wall. Mol Microbiol. 2007;66(5):1164–73. https://doi.org/10.1111/j.1365-2958.2007.05990.x.
32. Fernandes C, Gow NAR, Gonçalves T. The importance of subclasses of chitin synthase enzymes with myosin-like domains for the fitness of fungi. Fungal Biol Rev. 2016;30(1):1–14. https://doi.org/10.1016/j.fbr.2016.03.002.
33. Beauvais A, Schmidt C, Guadagnini S, Roux P, Perret E, Henry C, et al. An extracellular matrix glues together the aerial-grown hyphae of *Aspergillus fumigatus*. Cell Microbiol. 2007;9(6):1588–600. https://doi.org/10.1111/j.1462-5822.2007.00895.x.
34. Ruiz-Herrera J, San-Blas G. Chitin synthesis as target for antifungal drugs. Curr Drug Targets Infect Disord. 2003;3(1):77–91. https://doi.org/10.2174/1568005033342064.

35. Nicola AM, Albuquerque P, Paes HC, Fernandes L, Costa FF, Kioshima ES, et al. Antifungal drugs: new insights in research development. Pharmacol Ther. 2019;195:21–38. https://doi.org/10.1016/j.pharmthera.2018.10.008.
36. Wang J, Zhou L, Shi H, Chern M, Yu H, Yi H, et al. A single transcription factor promotes both yield and immunity in rice. Science. 2018;361(6406):1026–8. https://doi.org/10.1126/science.aat7675.
37. Wang N, Tang C, Fan X, He M, Gan P, Zhang S, Hu Z, et al. Inactivation of a wheat protein kinase gene confers broad-spectrum resistance to rust fungi. Cell. 2022;185(16):2961–74. https://doi.org/10.1016/j.cell.2022.06.027.
38. Oses-Ruiz M, Cruz-Mireles N, Martin-Urdiroz M, Soanes DM, Eseola AB, Tang B, et al. Appressorium-mediated plant infection by *Magnaporthe oryzae* is regulated by a Pmk1-dependent hierarchical transcriptional network. Nat Microbiol. 2021;6(11):1383–97. https://doi.org/10.1038/s41564-021-00978-w.
39. Li B, Liu LP, Li Y, Dong X, Zhang HF, Chen HG, et al. The FgVps39-FgVam7-FgSso1 complex mediates vesicle trafficking and is important for the development and virulence of *Fusarium graminearum*. Mol Plant Microbe Interact. 2017;30(5):410–22. https://doi.org/10.1094/MPMI-11-16-0242-R.
40. Liu MX, Hu JX, Zhang A, Dai Y, Chen WZ, He YL, et al. Auxilin-like protein MoSwa2 promotes effector secretion and virulence as a clathrin uncoating factor in the rice blast fungus *Magnaporthe oryzae*. New Phytol. 2021;230(2):720–36. https://doi.org/10.1111/nph.17181.
41. Li LW, Chen XL, Zhang SP, Yang J, Chen D, Liu MX, et al. MoCAP proteins regulated by MoArk1-mediated phosphorylation coordinate endocytosis and actin dynamics to govern development and virulence of *Magnaporthe oryzae*. PLoS Genet. 2017;13(5):e1006814. https://doi.org/10.1371/journal.pgen.1006814.
42. Jin X, Gou JY. A rapid and cost-effective fluorescence detection in tube (FDIT) method to analyze protein phosphorylation. Plant Methods. 2016;12:43. https://doi.org/10.1186/s13007-016-0143-5.
43. Wang JZ, Yin ZY, Tang W, Cai XJ, Gao CY, Zhang HF, et al. The thioredoxin MoTrx2 protein mediates reactive oxygen species (ROS) balance and controls pathogenicity as a target of the transcription factor MoAP1 in *Magnaporthe oryzae*. Mol Plant Pathol. 2017;18(9):1199–209. https://doi.org/10.1111/mpp.12484.
44. Huang L. Identification of direct transcriptional targets of CgCrzA under CFW conditions through Genome-wide ChIP-seq analysis. figshare; 2024. https://doi.org/10.6084/m9.figshare.26503291.
45. Huang L. LC-MS/MS analysis identified CgCrzA phosphorylation sites in the wild-type and Δ*Cgmkk1* mutant expressing CgCrzA.zip. figshare; 2024. https://doi.org/10.6084/m9.figshare.26500237.v1.

Publisher's Note